

Multi-symplectic Preserving Integrator for the Schrödinger Equation with Wave Operator

Linghua Kong^{a,*}, Lan Wang^a, Liying Zhang^b

^a*School of Mathematics and Information Science, Jiangxi Normal University,
Nanchang, Jiangxi, 330022, PR China*

^b*State Key Laboratory of Scientific and Engineering Computing,
Institute of Computational Mathematics and Scientific/Engineering Computing,
AMSS, CAS, P.O. Box 2719, Beijing, 100190, PR China*

Abstract

In the article, we discuss the conservation laws for the nonlinear Schrödinger equation with wave operator under multisymplectic integrator (MI). First, the conservation laws of the continuous equation are presented and one of them is new. The multisymplectic structure and MI are constructed for the equation. The discrete conservation laws of the numerical method are analyzed. It is verified that the proposed MI can stably simulate the multisymplectic Hamiltonian system excellent over long-term. It is more accurate than some energy-preserving schemes though they are of the same accuracy. Moreover, the residual of mass is less than energy-preserving schemes under the same mesh partition over long-term.

Keywords: Schrödinger equation with wave operator; Multisymplectic integrator; Conservation law.

2000 MSC: 65M06, 65M12, 65Z05, 70H15

1. Introduction

In this paper, we focus on the multisymplectic integrator (MI) for (1+1) nonlinear Schrödinger equations with wave operator (NLSEWO) [10]

$$\begin{cases} Wu - i\alpha u_t - i\theta u_x + \lambda u + \beta|u|^2 u = 0, & (x, t) \in [x_l, x_r] \times (0, T], \\ u(x, t) = u(x + (x_r - x_l), t), \\ u(x, 0) = f_0(x), \quad u_t(x, 0) = f_1(x), & x \in [x_l, x_r], \end{cases} \quad (1)$$

where $Wu = u_{tt} - u_{xx} + \gamma u_{tx}$, $i^2 = -1$, $\alpha, \gamma, \theta, \lambda$ and β are real constants, at the same time, $f_0(x)$ and $f_1(x)$ are given functions. The equation describes the nonlinear

*Corresponding author

Email addresses: konglh@mail.ustc.edu.cn (Linghua Kong), lyzhang@lsec.cc.ac.cn (Liying Zhang)

interaction between two quasi-monochromatic waves. It is one of the non-resonant interaction.

Proposition 1. *The determined problem (1) satisfies the following conservation laws*

- *Energy invariant*

$$\mathcal{E}(t) = \int_{x_l}^{x_r} (|u_t|^2 + |u_x|^2 + i\theta u \bar{u}_x + \lambda |u|^2 + \frac{\beta}{2} |u|^4) dx = \mathcal{E}(0). \quad (2)$$

- *Mass invariant*

$$\mathcal{Q}(t) = \int_{x_l}^{x_r} [(u_t \bar{u} - \bar{u}_t u) - \gamma u \bar{u}_x - i\alpha |u|^2] dx = \mathcal{Q}(0). \quad (3)$$

Proof: We multiply Eq. (1) with \bar{u}_t and integrate over spatial domain

$$\int_{x_l}^{x_r} (u_{tt} \bar{u}_t - u_{xx} \bar{u}_t + \gamma u_{tx} \bar{u}_t - i\alpha u_t \bar{u}_t - i\theta u_x \bar{u}_t + \lambda u \bar{u}_t + \beta |u|^2 u \bar{u}_t) dx = 0. \quad (4)$$

Next, we multiply the conjugation of Eq. (1) with u_t

$$\int_{x_l}^{x_r} (\bar{u}_{tt} u_t - \bar{u}_{xx} u_t + \gamma \bar{u}_{tx} u_t + i\alpha \bar{u}_t u_t + i\theta \bar{u}_x u_t + \lambda \bar{u} u_t + \beta |u|^2 \bar{u} u_t) dx = 0. \quad (5)$$

Adding Eq. (4) to Eq. (5) with integration by part under the boundary conditions, we have

$$\frac{d}{dt} \int_{x_l}^{x_r} \left[|u_t|^2 + |u_x|^2 + i\theta(u \bar{u}_x) + \lambda |u|^2 + \frac{\beta}{2} |u|^4 \right] dx = 0.$$

This is just what we desire. Consequently, we prove another invariant:

$$\begin{aligned} & \int_{x_l}^{x_r} [(u_{tt} \bar{u} - u_{xx} \bar{u} + \gamma u_{xt} \bar{u} - i\alpha u_t \bar{u} - i\theta u_x \bar{u} + \lambda |u|^2 + \beta |u|^4) \\ & \quad - (\bar{u}_{tt} u - \bar{u}_{xx} u + \gamma \bar{u}_{xt} u + i\alpha \bar{u}_t u + i\theta \bar{u}_x u + \lambda |u|^2 + \beta |u|^4)] dx \\ & = \frac{d}{dt} \int_{x_l}^{x_r} [(u_t \bar{u} - \bar{u}_t u) - \gamma(u \bar{u}_x) - i\alpha |u|^2] \\ & = 0. \end{aligned}$$

The proof is completed. □

It is noted that the mass invariant (3) is **new** which did not appear in existing literatures to our knowledge.

In [3], Guo proposed an implicit nonconservative difference scheme for NLSEWO. Based on the first conservative quantity, Zhang et al developed some energy-preserving schemes for it [18, 17, 16] in case of $\gamma = \theta = \lambda = 0$. Wang considered its Fourier pseudo-spectral method under multisymplectic context [13].

At the end of last century, MIs have been put forward and application to large numbers of partial differential equations, such as wave equation [2, 12, 15], nonlinear Schrödinger-type equations [4, 6], Dirac equation [5], Maxwell's equations [9], RLW equation [7]. The most important character of MIs is its multisymplecticity, and other conservative properties are preserved excellently despite of not exactly [1, 5, 8, 14, 19]. In the article, we investigate the MIs and its global conservative properties.

The rest of the paper is organized as follows: In Section 2, some preliminary knowledge is prepared for which will often be used later. In Section 3, it presents the multisymplectic structure and an MI for NLSEWO. The conservation properties of the proposed numerical schemes are investigated in Section 4. In Section 5, we present some numerical examples and detailed numerical results. Some conclusions are given to end this paper.

2. Preliminary Knowledge

In this section, we give some notations and knowledge we will frequently be used. A uniform partition of the domain under consideration is

$$x_k = x_l + kh, t_j = j\tau, k = 0, 1, 2, \dots, K; j = 0, 1, \dots, J.$$

Where $h = \frac{x_r - x_l}{K}$ and $\tau = \frac{T}{J}$ denote the spatial mesh size and temporal step length. u_k^j is an approximation of $u(x, t)$ at the node (x_k, t_j) , and $U_k^j = u(x_k, t_j)$. Some notations about difference quotient:

$$\begin{aligned} u_{kx}^j &= \frac{u_{k+1}^j - u_k^j}{h}, u_{k\bar{x}}^j = \frac{u_k^j - u_{k-1}^j}{h}, u_{k+\frac{1}{2}\hat{x}}^j = \frac{u_{k+1}^j - u_k^j}{h}, u_{k2x}^j = \frac{u_{k+1}^j - u_{k-1}^j}{2h}; \\ u_{kt}^j &= \frac{u_k^{j+1} - u_k^j}{\tau}, u_{k\bar{t}}^j = \frac{u_k^j - u_k^{j-1}}{\tau}, u_{k+\frac{1}{2}\hat{t}}^j = \frac{u_k^{j+1} - u_k^j}{\tau}, u_{k2t}^j = \frac{u_k^{j+1} - u_k^{j-1}}{2\tau}; \\ \delta_t^2 u_k^j &= \frac{u_k^{j+1} - 2u_k^j + u_k^{j-1}}{\tau^2}, \delta_x^2 u_k^j = \frac{u_{k+1}^j - 2u_k^j + u_{k-1}^j}{h^2}. \end{aligned}$$

For any vectors $u^j, v^j \in \mathbb{C}^K$, the inner product and norms are defined as:

$$\begin{aligned} \langle u^j, v^j \rangle &= h \sum_k u_k^j \bar{v}_k^j, \quad \|u^j\|^2 = \langle u^j, u^j \rangle, \\ \|u^j\|_{\frac{1}{2}}^2 &= h \sum_k \left| u_{k+\frac{1}{2}}^j \right|^2, \quad \|u^j\|_{\infty} = \max_k |u_k^j|. \end{aligned}$$

Lemma 1. *For all complex mesh functions $\{u_k^j\}$ and $\{v_k^j\}$ with periodic or homogeneous boundary condition, we have the following conclusions:*

- *Discrete Green formula:*

$$\langle \delta_x^2 u^j, v^j \rangle = -\langle \delta_x u^j, \delta_x v^j \rangle; \quad (6)$$

- $\langle \delta_{\bar{x}} u^j, u^j \rangle = -\langle u^j, \delta_{\bar{x}} u^j \rangle$ is purely imaginary.
- $Re \langle \delta_t^2 u^j, u_{2t}^j \rangle = \frac{1}{2} \|u_t^j\|_{\bar{t}}^2$, where ‘Re’ denotes taking real part.

These conclusion can be verified easily.

3. Construction of Multi-symplectic scheme

In this section, we firstly describe the multi-symplectic structure and local conservation laws for the Eq.(1). In order to rewrite the complex equations as a real one, we suppose that

$$\begin{cases} u(x, t) = \varphi(x, t) + i\psi(x, t), \\ u_t(x, t) = v(x, t) + iw(x, t), \\ u_x(x, t) = f(x, t) + ig(x, t), \end{cases}$$

where $\varphi(x, t), \psi(x, t), v(x, t), w(x, t), f(x, t), g(x, t)$ are all real-valued functions. Let $z = (\varphi, \psi, v, w, f, g)^T$, we have multi-symplectic equations

$$\begin{cases} \alpha\psi_t + v_t + \frac{\gamma}{2}f_t + \theta\psi_x + \frac{\gamma}{2}v_x - f_x = -\lambda\varphi - \beta(\varphi^2 + \psi^2)\varphi, \\ -\alpha\varphi_t + w_t + \frac{\gamma}{2}g_t - \theta\varphi_x + \frac{\gamma}{2}w_x - g_x = -\lambda\psi - \beta(\varphi^2 + \psi^2)\psi, \\ -\varphi_t - \frac{\gamma}{2}\varphi_x = -v - \frac{\gamma}{2}f, \\ -\psi_t - \frac{\gamma}{2}\psi_x = -w - \frac{\gamma}{2}g, \\ -\frac{\gamma}{2}\varphi_t + \varphi_x = -\frac{\gamma}{2}v + f, \\ -\frac{\gamma}{2}\psi_t + \psi_x = -\frac{\gamma}{2}w + g. \end{cases} \quad (7)$$

Then, we can cast (7) into the multi-symplectic framework

$$Mz_t + Kz_x = \nabla_z S(z), \quad (8)$$

where ∇ is the gradient operator. The Hamiltonian function is

$$S(z) = -\frac{1}{2}[\lambda(\varphi^2 + \psi^2) + \frac{\beta}{2}(\varphi^2 + \psi^2)^2 + v^2 + w^2 - (f^2 + g^2) + \gamma(vf + wg)].$$

$$M = \begin{bmatrix} 0 & \alpha & 1 & 0 & \frac{1}{2}\gamma & 0 \\ -\alpha & 0 & 0 & 1 & 0 & \frac{1}{2}\gamma \\ -1 & 0 & 0 & 0 & 0 & 0 \\ 0 & -1 & 0 & 0 & 0 & 0 \\ -\frac{\gamma}{2} & 0 & 0 & 0 & 0 & 0 \\ 0 & -\frac{\gamma}{2} & 0 & 0 & 0 & 0 \end{bmatrix}, \quad K = \begin{bmatrix} 0 & \theta & \frac{\gamma}{2} & 0 & -1 & 0 \\ -\theta & 0 & 0 & \frac{\gamma}{2} & 0 & -1 \\ -\frac{\gamma}{2} & 0 & 0 & 0 & 0 & 0 \\ 0 & -\frac{\gamma}{2} & 0 & 0 & 0 & 0 \\ 1 & 0 & 0 & 0 & 0 & 0 \\ 0 & 1 & 0 & 0 & 0 & 0 \end{bmatrix}.$$

According to the multi-symplectic theoretical background, the multi-symplectic system (8) satisfies local conservation laws as follows:

- Multi-symplectic conservation law

$$\frac{\partial}{\partial t}\omega + \frac{\partial}{\partial x}\kappa = 0, \quad \forall(x, t), \quad (9)$$

where ω and κ are pre-symplectic 2-forms

$$\begin{aligned} \omega &= \alpha d\varphi \wedge d\psi + d\varphi \wedge dv + \frac{\gamma}{2}d\varphi \wedge df + d\psi \wedge dw + \frac{\gamma}{2}d\psi \wedge dg, \\ \kappa &= \theta d\varphi \wedge d\psi - d\varphi \wedge df + \frac{\gamma}{2}d\varphi \wedge dv - d\psi \wedge dg + \frac{\gamma}{2}d\psi \wedge dw. \end{aligned}$$

- Local energy conservation law:

$$\frac{\partial}{\partial t}E(z) + \frac{\partial}{\partial x}F(z) = 0, \quad \forall(x, t), \quad (10)$$

where the energy density $E(z)$ and the energy flux $F(z)$ are

$$\begin{aligned} E(z) &= \frac{1}{2}[\lambda(\varphi^2 + \psi^2) + \frac{\beta}{2}(\varphi^2 + \psi^2)^2 + v^2 + w^2 + f^2 + g^2 + \theta(\varphi g - \psi f)], \\ F(z) &= \frac{\theta}{2}(\varphi w - \psi v) - \frac{\gamma}{2}(v^2 + w^2). \end{aligned}$$

- Local momentum conservation law:

$$\frac{\partial}{\partial t}I(z) + \frac{\partial}{\partial x}G(z) = 0, \quad (11)$$

where the momentum density $I(z)$ and the momentum flux $G(z)$ are

$$\begin{aligned} I(z) &= \frac{\alpha}{2}(\varphi g - \psi f) - (fv + gw) - \frac{\gamma}{2}(f^2 + g^2), \\ G(z) &= -\frac{\lambda}{2}(\varphi^2 + \psi^2) - \frac{\beta}{4}(\varphi^2 + \psi^2)^2 + \frac{1}{2}(v^2 + w^2 + f^2 + g^2) - \frac{\alpha}{2}(\varphi w - \psi v). \end{aligned}$$

It is well known that the local conservation laws imply that the density can be various, but the increment of the density in time puts up with the flux in space.

Applying the multisymplectic midpoint integrator

$$M\delta_{\hat{t}z_{k+\frac{1}{2}}}^{j+\frac{1}{2}} + K\delta_{\hat{x}z_{k+\frac{1}{2}}}^{j+\frac{1}{2}} = \nabla_z S(z_{k+\frac{1}{2}}^{j+\frac{1}{2}}), \quad (12)$$

where $z_{k+\frac{1}{2}}^{j+\frac{1}{2}} = \frac{1}{2}(z_{k+1}^{j+\frac{1}{2}} + z_k^{j+\frac{1}{2}}) = \frac{1}{2}(z_{k+\frac{1}{2}}^{j+1} + z_{k+\frac{1}{2}}^j) = \frac{1}{4}(z_{k+1}^{j+1} + z_{k+1}^j + z_k^{j+1} + z_k^j)$, to the multisymplectic Hamiltonian system (7), one has

$$\left\{ \begin{aligned} &\alpha\delta_{\hat{t}}\psi_{k+\frac{1}{2}}^{j+\frac{1}{2}} + \delta_{\hat{t}}v_{k+\frac{1}{2}}^{j+\frac{1}{2}} + \frac{\gamma}{2}\delta_{\hat{t}}f_{k+\frac{1}{2}}^{j+\frac{1}{2}} + \theta\delta_{\hat{x}}\psi_{k+\frac{1}{2}}^{j+\frac{1}{2}} + \frac{\gamma}{2}\delta_{\hat{x}}v_{k+\frac{1}{2}}^{j+\frac{1}{2}} - \delta_{\hat{x}}f_{k+\frac{1}{2}}^{j+\frac{1}{2}} \\ &= -\lambda\varphi_{k+\frac{1}{2}}^{j+\frac{1}{2}} - \beta \left[\left(\varphi_{k+\frac{1}{2}}^{j+\frac{1}{2}} \right)^2 + \left(\psi_{k+\frac{1}{2}}^{j+\frac{1}{2}} \right)^2 \right] \varphi_{k+\frac{1}{2}}^{j+\frac{1}{2}}, \\ &-\alpha\delta_{\hat{t}}\varphi_{k+\frac{1}{2}}^{j+\frac{1}{2}} + \delta_{\hat{t}}w_{k+\frac{1}{2}}^{j+\frac{1}{2}} + \frac{\gamma}{2}\delta_{\hat{t}}g_{k+\frac{1}{2}}^{j+\frac{1}{2}} - \theta\delta_{\hat{x}}\varphi_{k+\frac{1}{2}}^{j+\frac{1}{2}} + \frac{\gamma}{2}\delta_{\hat{x}}w_{k+\frac{1}{2}}^{j+\frac{1}{2}} - \delta_{\hat{x}}g_{k+\frac{1}{2}}^{j+\frac{1}{2}} \\ &= -\lambda\psi_{k+\frac{1}{2}}^{j+\frac{1}{2}} - \beta \left[\left(\varphi_{k+\frac{1}{2}}^{j+\frac{1}{2}} \right)^2 + \left(\psi_{k+\frac{1}{2}}^{j+\frac{1}{2}} \right)^2 \right] \psi_{k+\frac{1}{2}}^{j+\frac{1}{2}}, \\ &-\delta_{\hat{t}}\varphi_{k+\frac{1}{2}}^{j+\frac{1}{2}} = -v_{k+\frac{1}{2}}^{j+\frac{1}{2}}, \quad -\delta_{\hat{t}}\psi_{k+\frac{1}{2}}^{j+\frac{1}{2}} = -w_{k+\frac{1}{2}}^{j+\frac{1}{2}}, \\ &\delta_{\hat{x}}\varphi_{k+\frac{1}{2}}^{j+\frac{1}{2}} = f_{k+\frac{1}{2}}^{j+\frac{1}{2}}, \quad \delta_{\hat{x}}\psi_{k+\frac{1}{2}}^{j+\frac{1}{2}} = g_{k+\frac{1}{2}}^{j+\frac{1}{2}}. \end{aligned} \right. \quad (13)$$

For the details of the method and the theoretical results on local conservation laws of the numerical method, we refer to [5] and references therein.

The MI (13) is of second order both in time and space. After tedious calculation, by eliminating the introduced variables, it can be reformulated into

$$\begin{aligned} & \frac{1}{2}(\delta_t^2 u_{k+\frac{1}{2}}^j + \delta_t^2 u_{k-\frac{1}{2}}^j) - \frac{1}{2}(\delta_x^2 u_k^{j+\frac{1}{2}} + \delta_x^2 u_k^{j-\frac{1}{2}}) - \frac{i\alpha}{2}(\delta_{2t} u_{k+\frac{1}{2}}^j + \delta_{2t} u_{k-\frac{1}{2}}^j) \\ & - \frac{i\theta}{2}(\delta_{2x} u_k^{j+\frac{1}{2}} + \delta_{2x} u_k^{j-\frac{1}{2}}) + \gamma \delta_{2t} \delta_{2x} u_k^j + \frac{\lambda}{4} \left[u_{k+\frac{1}{2}}^{j+\frac{1}{2}} + u_{k-\frac{1}{2}}^{j+\frac{1}{2}} + u_{k+\frac{1}{2}}^{j-\frac{1}{2}} + u_{k-\frac{1}{2}}^{j-\frac{1}{2}} \right] \\ & + \frac{\beta}{4} \left[\left| u_{k+\frac{1}{2}}^{j+\frac{1}{2}} \right|^2 u_{k+\frac{1}{2}}^{j+\frac{1}{2}} + \left| u_{k+\frac{1}{2}}^{j-\frac{1}{2}} \right|^2 u_{k+\frac{1}{2}}^{j-\frac{1}{2}} + \left| u_{k-\frac{1}{2}}^{j+\frac{1}{2}} \right|^2 u_{k-\frac{1}{2}}^{j+\frac{1}{2}} + \left| u_{k-\frac{1}{2}}^{j-\frac{1}{2}} \right|^2 u_{k-\frac{1}{2}}^{j-\frac{1}{2}} \right] = 0. \end{aligned} \quad (14)$$

By Taylor expansion, the MI (14) is of second order both in space and time, that is, the truncation error is $\mathcal{T}_k^{j+\frac{1}{2}} = \mathcal{O}(\tau^2 + h^2)$.

4. Conservation Laws Analysis

In this section, the theoretical analysis about the MI (14) is derived. It is suggested that the MI can preserve the energy and mass very well though they are not exactly.

Firstly, we investigate the discrete energy conservation law. To the purpose, we multiply the Eq. (14) with

$$2 \left(\overline{u_k^{j+\frac{1}{2}}} - \overline{u_k^{j-\frac{1}{2}}} \right) = \overline{u_k^{j+1}} - \overline{u_k^{j-1}} = 2\tau \delta_{2t} \overline{u_k^j} = \tau (\delta_t \overline{u_k^{j+\frac{1}{2}}} + \delta_t \overline{u_k^{j-\frac{1}{2}}}),$$

and sum over index k . Then, from the third formulate in Lemma 1, one can obtain the real part of the first term is

$$\left\| \delta_t u^{j+\frac{1}{2}} \right\|_{\frac{1}{2}}^2 - \left\| \delta_t u^{j-\frac{1}{2}} \right\|_{\frac{1}{2}}^2. \quad (15)$$

By Green formula, the real part of the second term is

$$\begin{aligned} & -\frac{1}{2} \text{Re} \left\langle \delta_x^2 u^{j+\frac{1}{2}} + \delta_x^2 u^{j-\frac{1}{2}}, u^{j+\frac{1}{2}} - u^{j-\frac{1}{2}} \right\rangle \\ & = \text{Re} \left\langle \delta_{\bar{x}} u^{j+\frac{1}{2}} + \delta_{\bar{x}} u^{j-\frac{1}{2}}, \delta_{\bar{x}} u^{j+\frac{1}{2}} - \delta_{\bar{x}} u^{j-\frac{1}{2}} \right\rangle \\ & = \left\| \delta_{\bar{x}} u^{j+\frac{1}{2}} \right\|^2 - \left\| \delta_{\bar{x}} u^{j-\frac{1}{2}} \right\|^2. \end{aligned} \quad (16)$$

The third term

$$\begin{aligned} -\frac{i\alpha}{2} h \sum_k \left[\delta_{2t} u_{k+\frac{1}{2}}^j + \delta_{2t} u_{k-\frac{1}{2}}^j \right] 2\tau \delta_{2t} \overline{u_k^j} &= -2\tau i\alpha h \sum_k \left| \delta_{2t} u_{k+\frac{1}{2}}^j \right|^2 \\ &= -2\tau i\alpha \left\| \delta_{2t} u^j \right\|_{\frac{1}{2}}^2, \end{aligned}$$

is purely imaginary. Judged from the second conclusion of Lemma 1, the fifth term $\gamma h \sum_k (\delta_{2x} \delta_{2t} u_k^j) 2\tau \delta_{2t} \overline{u_k^j}$ is purely imaginary, too. Now, we analyze the fourth term

$$\begin{aligned}
& -\frac{i\theta}{2} h \sum_k (\delta_{2x} u_k^{j+\frac{1}{2}} + \delta_{2x} u_k^{j-\frac{1}{2}}) (\overline{u_k^{j+1}} - \overline{u_k^{j-1}}) \\
&= -i\theta h \sum_k (\delta_{2x} u_k^{j+\frac{1}{2}} + \delta_{2x} u_k^{j-\frac{1}{2}}) (\overline{u_k^{j+\frac{1}{2}}} - \overline{u_k^{j-\frac{1}{2}}}) \\
&= -\frac{i\theta}{2h} h \sum_k \left[(u_{k+1}^{j+\frac{1}{2}} + u_{k+1}^{j-\frac{1}{2}}) (\overline{u_k^{j+\frac{1}{2}}} - \overline{u_k^{j-\frac{1}{2}}}) - (u_k^{j+\frac{1}{2}} + u_k^{j-\frac{1}{2}}) (\overline{u_{k+1}^{j+\frac{1}{2}}} - \overline{u_{k+1}^{j-\frac{1}{2}}}) \right].
\end{aligned}$$

Its real part is

$$\begin{aligned}
& -\frac{i\theta}{2h} h \sum_k \left[(u_{k+1}^{j+\frac{1}{2}} \overline{u_k^{j+\frac{1}{2}}} - u_k^{j+\frac{1}{2}} \overline{u_{k+1}^{j+\frac{1}{2}}}) - (u_{k+1}^{j-\frac{1}{2}} \overline{u_k^{j-\frac{1}{2}}} - u_k^{j-\frac{1}{2}} \overline{u_{k+1}^{j-\frac{1}{2}}}) \right] \\
&= -\frac{i\theta}{2h} h \sum_k \left[(u_{k+1}^{j+\frac{1}{2}} \overline{u_k^{j+\frac{1}{2}}} - u_{k+1}^{j+\frac{1}{2}} \overline{u_{k+1}^{j+\frac{1}{2}}}) - (u_k^{j+\frac{1}{2}} \overline{u_{k+1}^{j+\frac{1}{2}}} - u_k^{j+\frac{1}{2}} \overline{u_k^{j+\frac{1}{2}}}) \right. \\
&\quad \left. - (u_{k+1}^{j-\frac{1}{2}} \overline{u_k^{j-\frac{1}{2}}} - u_{k+1}^{j-\frac{1}{2}} \overline{u_{k+1}^{j-\frac{1}{2}}}) + (u_k^{j-\frac{1}{2}} \overline{u_{k+1}^{j-\frac{1}{2}}} - u_k^{j-\frac{1}{2}} \overline{u_k^{j-\frac{1}{2}}}) \right] \\
&= i\theta h \sum_k \left[u_{k+\frac{1}{2}}^{j+\frac{1}{2}} \overline{\delta_{\hat{x}} u_{k+\frac{1}{2}}^{j+\frac{1}{2}}} - u_{k+\frac{1}{2}}^{j-\frac{1}{2}} \overline{\delta_{\hat{x}} u_{k+\frac{1}{2}}^{j-\frac{1}{2}}} \right].
\end{aligned} \tag{17}$$

The real part of the sixth term reads

$$\begin{aligned}
& \frac{2\lambda}{4} h \operatorname{Re} \sum_k \left[\left(u_{k+\frac{1}{2}}^{j+\frac{1}{2}} + u_{k+\frac{1}{2}}^{j-\frac{1}{2}} \right) + \left(u_{k-\frac{1}{2}}^{j+\frac{1}{2}} + u_{k-\frac{1}{2}}^{j-\frac{1}{2}} \right) \right] \left(\overline{u_k^{j+\frac{1}{2}}} - \overline{u_k^{j-\frac{1}{2}}} \right) \\
&= \lambda h \operatorname{Re} \sum_k \left(u_{k+\frac{1}{2}}^{j+\frac{1}{2}} + u_{k+\frac{1}{2}}^{j-\frac{1}{2}} \right) \left(\overline{u_{k+\frac{1}{2}}^{j+\frac{1}{2}}} - \overline{u_{k+\frac{1}{2}}^{j-\frac{1}{2}}} \right) \\
&= \lambda \left(\left\| u^{j+\frac{1}{2}} \right\|_{\frac{1}{2}}^2 - \left\| u^{j-\frac{1}{2}} \right\|_{\frac{1}{2}}^2 \right).
\end{aligned} \tag{18}$$

The last term is

$$\begin{aligned}
& \frac{2\beta}{4} h \sum_k \left[\left| u_{k+\frac{1}{2}}^{j+\frac{1}{2}} \right|^2 u_{k+\frac{1}{2}}^{j+\frac{1}{2}} + \left| u_{k+\frac{1}{2}}^{j-\frac{1}{2}} \right|^2 u_{k+\frac{1}{2}}^{j-\frac{1}{2}} + \left| u_{k-\frac{1}{2}}^{j+\frac{1}{2}} \right|^2 u_{k-\frac{1}{2}}^{j+\frac{1}{2}} + \left| u_{k-\frac{1}{2}}^{j-\frac{1}{2}} \right|^2 u_{k-\frac{1}{2}}^{j-\frac{1}{2}} \right] \left[\overline{u_k^{j+\frac{1}{2}}} - \overline{u_k^{j-\frac{1}{2}}} \right] \\
&= \beta h \sum_k \left[\left| u_{k+\frac{1}{2}}^{j+\frac{1}{2}} \right|^2 u_{k+\frac{1}{2}}^{j+\frac{1}{2}} + \left| u_{k+\frac{1}{2}}^{j-\frac{1}{2}} \right|^2 u_{k+\frac{1}{2}}^{j-\frac{1}{2}} \right] \left[\overline{u_{k+\frac{1}{2}}^{j+\frac{1}{2}}} - \overline{u_{k+\frac{1}{2}}^{j-\frac{1}{2}}} \right] \\
&= \beta h \sum_k \left[\left| u_{k+\frac{1}{2}}^{j+\frac{1}{2}} \right|^4 - \left| u_{k+\frac{1}{2}}^{j-\frac{1}{2}} \right|^4 + \left| u_{k+\frac{1}{2}}^{j-\frac{1}{2}} \right|^2 u_{k+\frac{1}{2}}^{j-\frac{1}{2}} \overline{u_{k+\frac{1}{2}}^{j+\frac{1}{2}}} - \left| u_{k+\frac{1}{2}}^{j+\frac{1}{2}} \right|^2 u_{k+\frac{1}{2}}^{j+\frac{1}{2}} \overline{u_{k+\frac{1}{2}}^{j-\frac{1}{2}}} \right],
\end{aligned}$$

with the real part

$$\begin{aligned}
& 2\frac{\beta}{2} \left[\left\| u^{j+\frac{1}{2}} \right\|_{\frac{1}{2}}^4 - \left\| u^{j-\frac{1}{2}} \right\|_{\frac{1}{2}}^4 \right] + \beta h \operatorname{Re} \sum_k \left(\left| u_{k+\frac{1}{2}}^{j-\frac{1}{2}} \right|^2 u_{k+\frac{1}{2}}^{j-\frac{1}{2}} \overline{u_{k+\frac{1}{2}}^{j+\frac{1}{2}}} - \left| u_{k+\frac{1}{2}}^{j+\frac{1}{2}} \right|^2 u_{k+\frac{1}{2}}^{j+\frac{1}{2}} \overline{u_{k+\frac{1}{2}}^{j-\frac{1}{2}}} \right) \\
&= \frac{\beta}{2} \left[\left\| u^{j+\frac{1}{2}} \right\|_{\frac{1}{2}}^4 - \left\| u^{j-\frac{1}{2}} \right\|_{\frac{1}{2}}^4 \right] + \frac{\beta}{2} h \sum_k \left[\left| u_{k+\frac{1}{2}}^{j+\frac{1}{2}} \right|^2 - \left| u_{k+\frac{1}{2}}^{j-\frac{1}{2}} \right|^2 \right] \left| u_{k+\frac{1}{2}}^{j+\frac{1}{2}} - u_{k+\frac{1}{2}}^{j-\frac{1}{2}} \right|^2.
\end{aligned}$$

In summary, one has the following theorem:

Theorem 1. *The Preissman MI (14) possesses the discrete implicit energy conservation law, i.e.*

$$\mathcal{E}^{j+\frac{1}{2}} - \mathcal{E}^{j-\frac{1}{2}} = -\frac{\beta}{2}h \sum_k \left[\left| u_{k+\frac{1}{2}}^{j+\frac{1}{2}} \right|^2 - \left| u_{k+\frac{1}{2}}^{j-\frac{1}{2}} \right|^2 \right] \left| \delta_{2t} u_{k+\frac{1}{2}}^j \right|^2 \tau^2, \quad (19)$$

where $\mathcal{E}^{j+\frac{1}{2}} = \|\delta_t u^{j+\frac{1}{2}}\|_{\frac{1}{2}}^2 + i\theta h \sum_k u_{k+\frac{1}{2}}^{j+\frac{1}{2}} \overline{\delta_{\bar{x}} u_{k+\frac{1}{2}}^{j+\frac{1}{2}}} + \|\delta_{\bar{x}} u^{j+\frac{1}{2}}\|_{\frac{1}{2}}^2 + \lambda \left\| u^{j+\frac{1}{2}} \right\|_{\frac{1}{2}}^2 + \frac{\beta}{2} \left\| u^{j+\frac{1}{2}} \right\|_{\frac{1}{2}}^4$. In particular, in case of $\beta = 0$, the conservation law is explicit, that is,

$$\mathcal{E}^{j+\frac{1}{2}} = \mathcal{E}^{j-\frac{1}{2}} = \dots = \mathcal{E}^{\frac{1}{2}}. \quad (20)$$

Furthermore, we have the implicit mass conservation law:

Theorem 2. *The Preissman MI (14) admits the implicit mass conservation law*

$$\begin{aligned} & \frac{\mathcal{Q}^{j+\frac{1}{2}} - \mathcal{Q}^{j-\frac{1}{2}}}{\tau} \\ &= -\frac{\beta}{2}h \sum_k \left[\left| u_{k+\frac{1}{2}}^{j+\frac{1}{2}} \right|^2 - \left| u_{k+\frac{1}{2}}^{j-\frac{1}{2}} \right|^2 \right] \left(u_{k+\frac{1}{2}}^{j+\frac{1}{2}} - u_{k+\frac{1}{2}}^{j-\frac{1}{2}} \right) \left(\overline{u_{k+\frac{1}{2}}^{j+\frac{1}{2}}} + \overline{u_{k+\frac{1}{2}}^{j-\frac{1}{2}}} \right) \\ & \quad + \frac{\beta}{2}h \sum_k \left[\left| u_{k+\frac{1}{2}}^{j+\frac{1}{2}} \right|^2 - \left| u_{k+\frac{1}{2}}^{j-\frac{1}{2}} \right|^2 \right]^2, \end{aligned} \quad (21)$$

where $\mathcal{Q}^{j+\frac{1}{2}} = h \sum_k \left[\delta_t u_{k+\frac{1}{2}}^{j+\frac{1}{2}} \overline{u_{k+\frac{1}{2}}^{j+\frac{1}{2}}} - u_{k+\frac{1}{2}}^{j+\frac{1}{2}} \overline{\delta_t u_{k+\frac{1}{2}}^{j+\frac{1}{2}}} \right] - \gamma h \sum_k u_{k+\frac{1}{2}}^{j+\frac{1}{2}} \overline{\delta_{\bar{x}} u_{k+\frac{1}{2}}^{j+\frac{1}{2}}} - i\alpha \left\| u^{j+\frac{1}{2}} \right\|^2$. In particular, if $\beta = 0$, the conservation law is explicit, that is,

$$\mathcal{Q}^{j+\frac{1}{2}} = \mathcal{Q}^{j-\frac{1}{2}} = \dots = \mathcal{Q}^{\frac{1}{2}}. \quad (22)$$

Proof: Taking inner product of (14) with

$$Bu_k^j = u_k^{j+1} + 2u_k^j + u_k^{j-1} = 2(u_k^{j+\frac{1}{2}} + u_k^{j-\frac{1}{2}}),$$

the first term is showed as

$$\begin{aligned} & \frac{1}{2}h \sum_k (\delta_t^2 u_{k+\frac{1}{2}}^j + \delta_t^2 u_{k-\frac{1}{2}}^j) (\overline{u_k^{j+1}} + 2\overline{u_k^j} + \overline{u_k^{j-1}}) \\ &= \frac{1}{\tau^2}h \sum_k \left[(u_{k+\frac{1}{2}}^{j+1} - u_{k+\frac{1}{2}}^j) - (u_{k+\frac{1}{2}}^j - u_{k+\frac{1}{2}}^{j-1}) \right] \left[(\overline{u_{k+\frac{1}{2}}^{j+1}} + \overline{u_{k+\frac{1}{2}}^j}) + (\overline{u_{k+\frac{1}{2}}^j} + \overline{u_{k+\frac{1}{2}}^{j-1}}) \right], \end{aligned}$$

whose imaginary part is as follows:

$$\begin{aligned} & \frac{2}{\tau^2}h \sum_k \left[u_{k+\frac{1}{2}}^{j+1} \overline{u_{k+\frac{1}{2}}^j} - \overline{u_{k+\frac{1}{2}}^{j+1}} u_{k+\frac{1}{2}}^j - u_{k+\frac{1}{2}}^j \overline{u_{k+\frac{1}{2}}^{j-1}} + \overline{u_{k+\frac{1}{2}}^j} u_{k+\frac{1}{2}}^{j-1} \right] \\ &= \frac{2}{\tau}h \sum_k \left[\left(\delta_t u_{k+\frac{1}{2}}^{j+\frac{1}{2}} \overline{u_{k+\frac{1}{2}}^{j+\frac{1}{2}}} - \overline{\delta_t u_{k+\frac{1}{2}}^{j+\frac{1}{2}}} u_{k+\frac{1}{2}}^{j+\frac{1}{2}} \right) - \left(\delta_t u_{k+\frac{1}{2}}^{j-\frac{1}{2}} \overline{u_{k+\frac{1}{2}}^{j-\frac{1}{2}}} - \overline{\delta_t u_{k+\frac{1}{2}}^{j-\frac{1}{2}}} u_{k+\frac{1}{2}}^{j-\frac{1}{2}} \right) \right]. \end{aligned} \quad (23)$$

The second term

$$-\frac{1}{2}h \sum_k \delta_x^2 \left(u_k^{j+\frac{1}{2}} + u_k^{j-\frac{1}{2}} \right) B\bar{u}_k^j = -\frac{1}{4}h \sum_k \delta_x^2 B u_k^j B \bar{u}_k^j = \frac{1}{4}h \sum_k \left| \delta_{\bar{x}}(B u_k^j) \right|^2,$$

is real. The fourth term

$$-\frac{i\theta}{4}h \sum_k \delta_{2x} B u_k^j B \bar{u}_k^j = -\frac{i\theta}{8h}h \sum_k \left(B u_{k+1}^j B \bar{u}_k^j - B u_{k-1}^j B \bar{u}_k^j \right),$$

and the sixth term

$$\begin{aligned} & \frac{\lambda}{4}h \sum_k \left[\left(u_{k+\frac{1}{2}}^{j+\frac{1}{2}} + u_{k+\frac{1}{2}}^{j-\frac{1}{2}} \right) + \left(u_{k-\frac{1}{2}}^{j+\frac{1}{2}} + u_{k-\frac{1}{2}}^{j-\frac{1}{2}} \right) \right] 2 \left[\overline{u_k^{j+\frac{1}{2}}} + \overline{u_k^{j-\frac{1}{2}}} \right] \\ &= \lambda h \sum_k \left| u_{k+\frac{1}{2}}^{j+\frac{1}{2}} + u_{k+\frac{1}{2}}^{j-\frac{1}{2}} \right|^2, \end{aligned}$$

are real, too. The third term is

$$\begin{aligned} & i\alpha h \sum_k \left(\delta_{2t} u_{k+\frac{1}{2}}^j + \delta_{2t} u_{k-\frac{1}{2}}^j \right) \left(\overline{u_k^{j+\frac{1}{2}}} + \overline{u_k^{j-\frac{1}{2}}} \right) \\ &= -\frac{2i\alpha}{\tau}h \sum_k \left(u_{k+\frac{1}{2}}^{j+\frac{1}{2}} - u_{k+\frac{1}{2}}^{j-\frac{1}{2}} \right) \left(\overline{u_{k+\frac{1}{2}}^{j+\frac{1}{2}}} + \overline{u_{k+\frac{1}{2}}^{j-\frac{1}{2}}} \right). \end{aligned}$$

Abstract the imaginary part from this term, one obtains

$$-\frac{2\alpha i}{\tau} \left(\left\| u^{j+\frac{1}{2}} \right\|_{\frac{1}{2}}^2 - \left\| u^{j-\frac{1}{2}} \right\|_{\frac{1}{2}}^2 \right). \quad (24)$$

Now, we analyze the fifth term

$$\begin{aligned} & \gamma \delta_{2t} \delta_{2x} u_k^j \left(\overline{u_k^{j+1}} + 2\overline{u_k^j} + \overline{u_k^{j-1}} \right) \\ &= \frac{2\gamma}{h\tau}h \sum_k \left[\left(u_{k+\frac{1}{2}}^{j+\frac{1}{2}} - u_{k+\frac{1}{2}}^{j-\frac{1}{2}} \right) - \left(u_{k-\frac{1}{2}}^{j+\frac{1}{2}} - u_{k-\frac{1}{2}}^{j-\frac{1}{2}} \right) \right] \left(\overline{u_k^{j+\frac{1}{2}}} + \overline{u_k^{j-\frac{1}{2}}} \right) \\ &= -\frac{2\gamma}{h\tau}h \sum_k \left(u_{k+1}^{j+\frac{1}{2}} - u_{k+1}^{j-\frac{1}{2}} \right) \left[\left(\overline{u_{k+1}^{j+\frac{1}{2}}} + \overline{u_{k+1}^{j-\frac{1}{2}}} \right) - \left(\overline{u_k^{j+\frac{1}{2}}} + \overline{u_k^{j-\frac{1}{2}}} \right) \right] \\ &= -\frac{2\gamma}{\tau}h \sum_k \left(u_{k+1}^{j+\frac{1}{2}} - u_{k+1}^{j-\frac{1}{2}} \right) \left(\delta_{\hat{x}} \overline{u_{k+\frac{1}{2}}^{j+\frac{1}{2}}} + \delta_{\hat{x}} \overline{u_{k+\frac{1}{2}}^{j-\frac{1}{2}}} \right) \\ &= -\frac{2\gamma}{\tau}h \sum_k \left(u_{k+\frac{1}{2}}^{j+\frac{1}{2}} \delta_{\hat{x}} \overline{u_{k+\frac{1}{2}}^{j+\frac{1}{2}}} - u_{k+\frac{1}{2}}^{j-\frac{1}{2}} \delta_{\hat{x}} \overline{u_{k+\frac{1}{2}}^{j-\frac{1}{2}}} \right) \\ & \quad - \frac{2\gamma}{\tau}h \sum_k \left(u_{k+\frac{1}{2}}^{j+\frac{1}{2}} \delta_{\hat{x}} \overline{u_{k+\frac{1}{2}}^{j-\frac{1}{2}}} - u_{k+\frac{1}{2}}^{j-\frac{1}{2}} \delta_{\hat{x}} \overline{u_{k+\frac{1}{2}}^{j+\frac{1}{2}}} \right). \end{aligned}$$

Based on the second conclusion in Lemma 1, the first part of the above equality is purely imaginary, and the second part is real. Therefore, the imaginary part of the term is

$$-\frac{2\gamma}{\tau}h \sum_k \left(u_{k+\frac{1}{2}}^{j+\frac{1}{2}} \overline{\delta_{\hat{x}} u_{k+\frac{1}{2}}^{j+\frac{1}{2}}} - u_{k+\frac{1}{2}}^{j-\frac{1}{2}} \overline{\delta_{\hat{x}} u_{k+\frac{1}{2}}^{j-\frac{1}{2}}} \right). \quad (25)$$

Finally, the last term is

$$\begin{aligned} & \frac{2\beta}{4}h \sum_k \left(\left| u_{k+\frac{1}{2}}^{j+\frac{1}{2}} \right|^2 u_{k+\frac{1}{2}}^{j+\frac{1}{2}} + \left| u_{k+\frac{1}{2}}^{j-\frac{1}{2}} \right|^2 u_{k+\frac{1}{2}}^{j-\frac{1}{2}} + \left| u_{k-\frac{1}{2}}^{j+\frac{1}{2}} \right|^2 u_{k-\frac{1}{2}}^{j+\frac{1}{2}} + \left| u_{k-\frac{1}{2}}^{j-\frac{1}{2}} \right|^2 u_{k-\frac{1}{2}}^{j-\frac{1}{2}} \right) \left(\overline{u_k^{j+\frac{1}{2}}} + \overline{u_k^{j-\frac{1}{2}}} \right) \\ &= \frac{\beta}{2}h \sum_k \left(\left| u_{k+\frac{1}{2}}^{j+\frac{1}{2}} \right|^2 u_{k+\frac{1}{2}}^{j+\frac{1}{2}} + \left| u_{k+\frac{1}{2}}^{j-\frac{1}{2}} \right|^2 u_{k+\frac{1}{2}}^{j-\frac{1}{2}} \right) \left(\overline{u_{k+\frac{1}{2}}^{j+\frac{1}{2}}} + \overline{u_{k+\frac{1}{2}}^{j-\frac{1}{2}}} \right). \end{aligned}$$

The imaginary part this term is

$$\begin{aligned} & \frac{\beta}{2}\mathcal{I}h \sum_k \left(\left| u_{k+\frac{1}{2}}^{j+\frac{1}{2}} \right| u_{k+\frac{1}{2}}^{j+\frac{1}{2}} \overline{u_{k+\frac{1}{2}}^{j-\frac{1}{2}}} + \left| u_{k+\frac{1}{2}}^{j-\frac{1}{2}} \right| u_{k+\frac{1}{2}}^{j-\frac{1}{2}} \overline{u_{k+\frac{1}{2}}^{j+\frac{1}{2}}} \right) \\ &= \frac{\beta}{4}h \sum_k \left[\left| u_{k+\frac{1}{2}}^{j+\frac{1}{2}} \right|^2 - \left| u_{k+\frac{1}{2}}^{j-\frac{1}{2}} \right|^2 \right] \left[u_{k+\frac{1}{2}}^{j+\frac{1}{2}} \overline{u_{k+\frac{1}{2}}^{j-\frac{1}{2}}} - u_{k+\frac{1}{2}}^{j-\frac{1}{2}} \overline{u_{k+\frac{1}{2}}^{j+\frac{1}{2}}} \right] \\ &= \frac{\beta}{4}h \sum_k \left[\left| u_{k+\frac{1}{2}}^{j+\frac{1}{2}} \right|^2 - \left| u_{k+\frac{1}{2}}^{j-\frac{1}{2}} \right|^2 \right] \left(u_{k+\frac{1}{2}}^{j+\frac{1}{2}} - u_{k+\frac{1}{2}}^{j-\frac{1}{2}} \right) \left(\overline{u_{k+\frac{1}{2}}^{j+\frac{1}{2}}} + \overline{u_{k+\frac{1}{2}}^{j-\frac{1}{2}}} \right) \\ & \quad - \frac{\beta}{4}h \sum_k \left[\left| u_{k+\frac{1}{2}}^{j+\frac{1}{2}} \right|^2 - \left| u_{k+\frac{1}{2}}^{j-\frac{1}{2}} \right|^2 \right]^2. \end{aligned} \quad (26)$$

Summing over the equalities (23), (24), (25) and (26), one obtains the conclusion what one wishes. \square

5. Numerical examples

In this section, we investigate the theoretical analysis by a series of numerical experiments, including conservation properties and the accuracy of the schemes.

Example 1. Firstly, we consider a linear problem, i.e., $\beta = 0$,

$$\begin{cases} u_{tt} - u_{xx} + u_{tx} + i(u_t + u_x) + 3u = 0, & (x, t) \in [0, 2\pi] \times (0, 50], \\ u(x + 2\pi, t) = u(x, t), u(x, 0) = \exp(ix), u_t(x, 0) = -3i \exp(ix). \end{cases} \quad (27)$$

In this case, the energy and mass are constants from Theorems 1 and 2. The exact solution of the determined problem is

$$u(x, t) = \exp(i(x - 3t)), \quad (28)$$

which is a plane wave propagating to the right with velocity $v = 3$. The amplitude of the wave is equal to 1. We simulate the problem by the MI (14) under diverse mesh

divisions. The left of Fig. 1 shows the maximum error for the real part of numerical solution against the space mesh numbers under $\tau = 0.005$ at $t = 50$, and the right one presents the maximum error for the imaginary part of numerical solution against the time mesh numbers under $h = \frac{2\pi}{1024}$ at $t = 50$. The error is metered $e = u_k^j - U_k^j$. The figures imply that the numerical solution of the MI (14) converges to the exact solution almost with the same rate 2 both in time and space. Fig. 2 presents the phasic profiles of the numerical solution at every time step. It is suggested that the curves are overlapped and always keep a unit circle. This exactly agrees with the exact solution (28). Fig. 3 plots the residuals of energy (left) and mass (right) with $\tau = 0.01, h = \frac{2\pi}{64}$ against time $t \in [0, 1000]$. Judging from the plots, the MI preserves both the energy and mass indeed in case of $\beta = 0$.

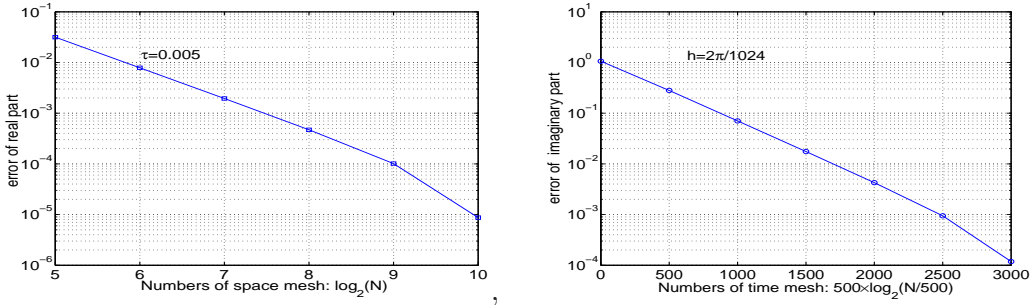


Figure 1: Numerical error vs. mesh numbers: left for space, right for time.

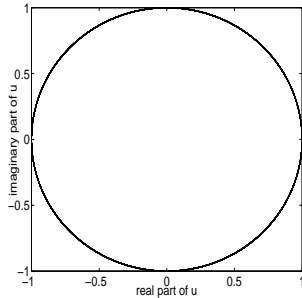


Figure 2: Phasic profiles of numerical solution at all time steps.

Example 2. We simulate the following problem

$$\begin{cases} u_{tt} - u_{xx} + u_{tx} + i(u_t + u_x) + u + 2|u|^2u = 0, & (x, t) \in [0, 2\pi] \times (0, 200], \\ u(x + 2\pi, t) = u(x, t), & u(x, 0) = \exp(ix), \quad u_t(x, 0) = i \exp(ix), \end{cases} \quad (29)$$

by MI (14) until $T = 200$. The problem admits the following exact solution

$$u(x, t) = \exp(i(x + t)). \quad (30)$$

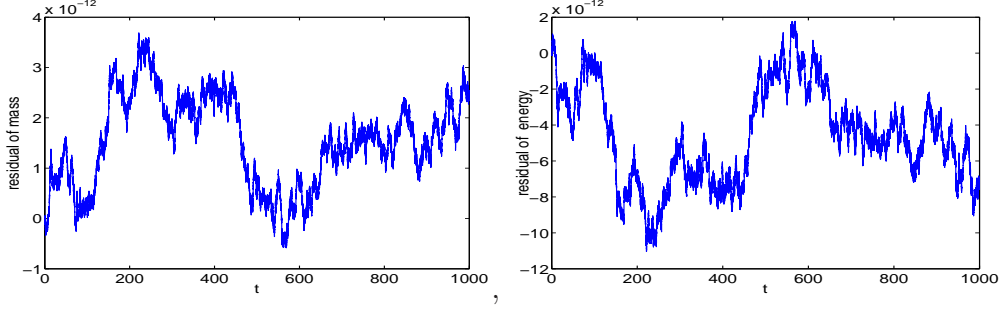


Figure 3: Residuals of mass (left) and energy (right).

The spatial-temporal domain is divided by $\tau = 0.01$, $h = \frac{\pi}{100}$. The real and imaginary part of the numerical solution at different time are profiled in Fig. 4, and the residuals of mass and energy against time are presented in Fig. 5. From the figures, we can find that the curves of the real part always follow cosine evolution, and the imaginary part are sine. The residuals of mass and energy take on periodic evolution. It is very interesting that the residual plots of the mass and energy are very like.

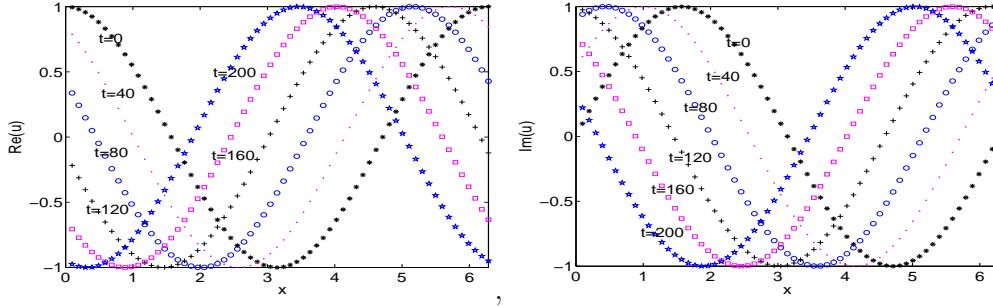


Figure 4: The real (left) and imaginary (right) parts of the numerical solution at different times.

Example 3. Next, we test the periodic initial valued problem

$$\begin{cases} u_{tt} - u_{xx} + iu_t + 2|u|^2u = 0, & (x, t) \in [0, 2\pi] \times (0, 100], \\ u(x + 2\pi, t) = u(x, t), \\ u(x, 0) = \sqrt{3}\exp(6ix), \quad u_t(x, 0) = -7\sqrt{3}i\exp(6ix), \end{cases} \quad (31)$$

We simulate the problem by the MI (14) and Wang's energy preserving scheme

$$\delta_t^2 u_k^j - \frac{1}{2}(\delta_x^2 u_k^{j+1} + \delta_x^2 u_k^{j-1}) + i\alpha\delta_t u_k^j + (|u_k^{j+1}|^2 + |u_k^{j-1}|^2)\frac{u_k^{j+1} + u_k^{j-1}}{2} = 0. \quad (32)$$

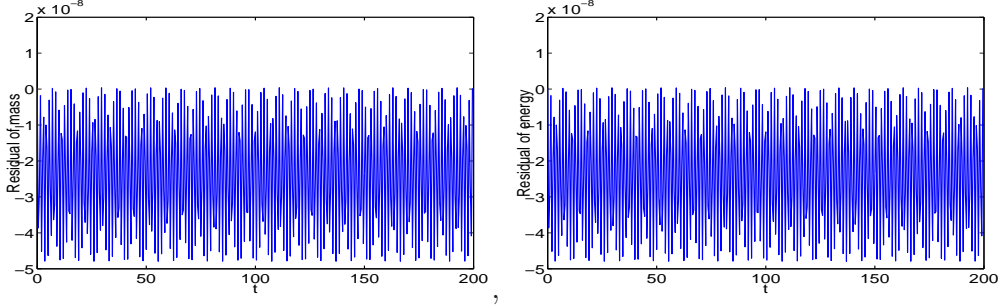


Figure 5: The residuals of mass (left) and energy (right).

This scheme preserves the energy (2) exactly [17], that is,

$$\mathcal{E}^n = \|(u_k^j)_t\|^2 + \frac{1}{2} \left(\|(u_k^{j+1})_x\|^2 + \|(u_k^j)_x\|^2 \right) + h \sum_k |u_k^j|^4 = \mathcal{E}^0. \quad (33)$$

We take $T = 100$, $h = \frac{2\pi}{200}$, $\tau = 0.01$ in the example. The error of numerical solution which is measured $e_\infty = \max_k | |u_k^j|^2 - |u(x_k, t_j)|^2 |$ by schemes (14) and (32) is presented in Fig. 6, and the comparison of the conservative properties is plotted in Fig. 7.

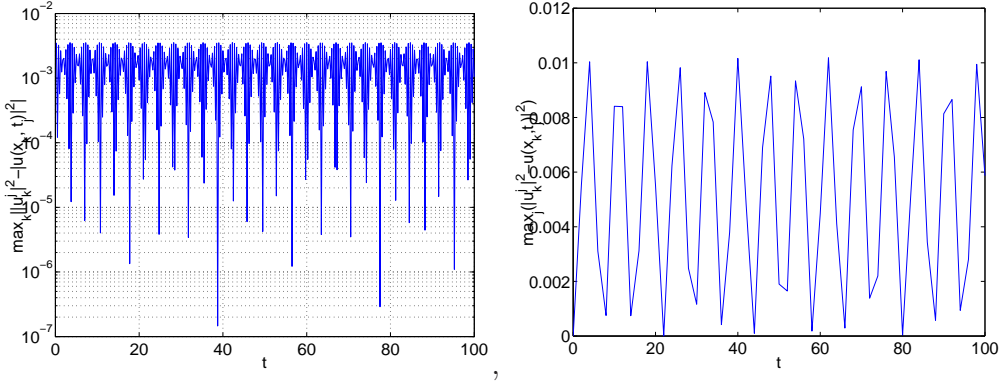


Figure 6: Comparison e_∞ by schemes (14) and (32). Left for scheme (14), right for (32).

From the figures, we can observe the following phenomena: i) The numerical solution of the multisymplectic scheme (14) is more accurate than that of Wang's scheme (32) in the test. ii) Wang's scheme (32) preserves the energy up to 10^{-10} scale, but not mass. The residuals of energy and mass for multisymplectic scheme (14) are fluctuated periodically, furthermore, they are very small relatively to their exact values, up to 10^{-7} and 10^{-4} scale, respectively.

Example 4. In the example, we consider the following problem[16]

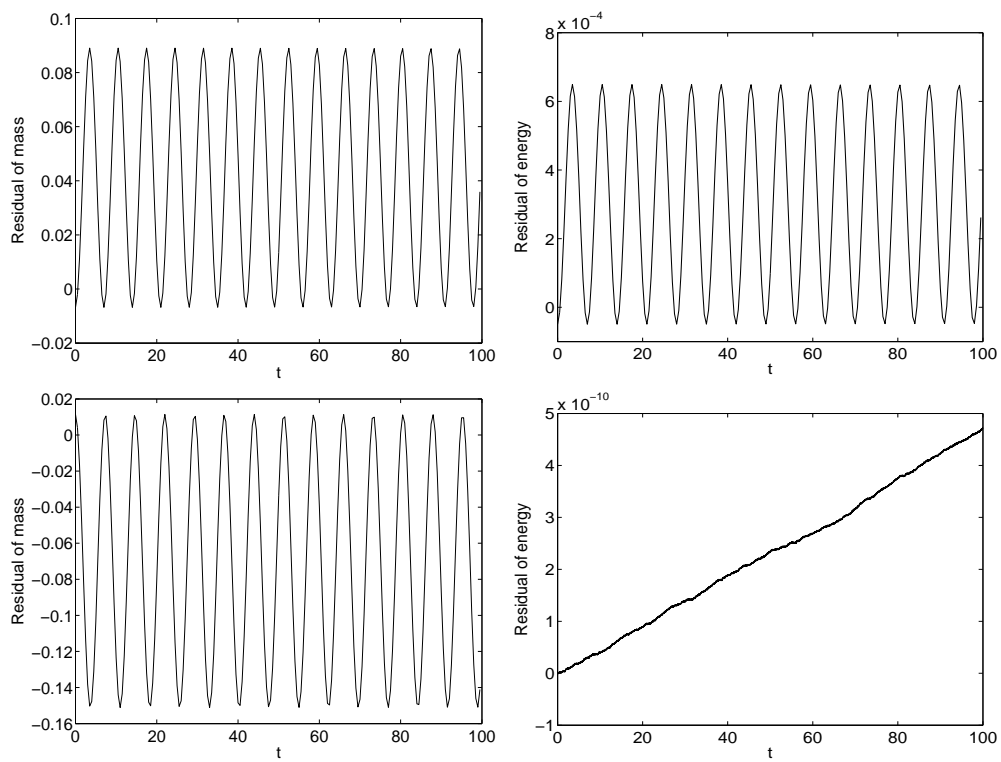


Figure 7: Conservative comparison. Upper for scheme (14), lower for scheme (32). Left for mass, right for energy.

$$\begin{cases} u_{tt} - u_{xx} + iu_t + 2|u|^2u = 0, & (x, t) \in [-50, 50] \times (0, 500], \\ u(x, 0) = A \operatorname{sech}(Kx), \quad u_t(x, 0) = i\nu A \operatorname{sech}(Kx). \end{cases} \quad (34)$$

The problem has the solution in the form

$$u(x, t) = A \operatorname{sech}(Kx) \exp(i\nu t), \quad (35)$$

where $A = |K|$, $\nu = \frac{1}{2}(-1 \pm \sqrt{1 - 4K^2})$.

We take $K = \frac{1}{4}$, $\nu = -\frac{1}{2} - \frac{\sqrt{3}}{4}$ in the test.

The spatial-temporal domain is partitioned by $h = 0.1$, $\tau = 0.05$. The numerical results are reported in Figs. 8-10. Fig. 8 is the solitary wave shape of $|u|$ and its contour by MI (14). Fig. 9 is the error of the real part of the numerical solution by schemes (14) and (32), and Fig. 10 is the residuals of conservative quantities. Here we have omitted the counterpart of Fig. 8 by scheme (32) and the error of imaginary part because they are very similar.

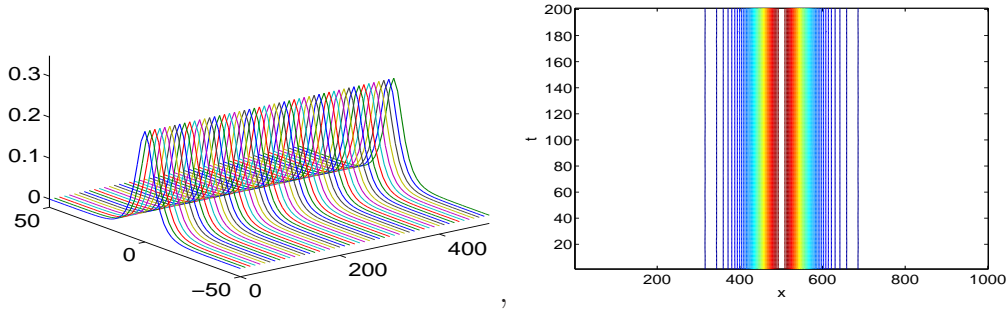


Figure 8: The solitary wave shape (left) and contours (right) of $|u|$ by scheme (14).

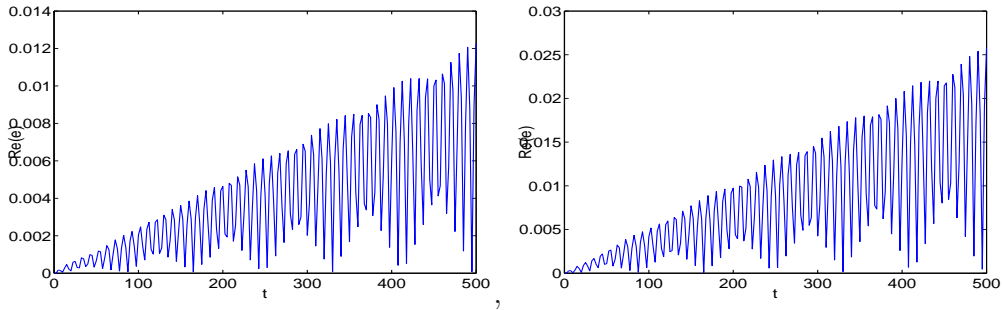


Figure 9: Comparison $Re(e) = \max_k | |u_k^j| - |u(x_k, t_j)| |$ by schemes (14) and (32). Left for scheme (14), right for (32).

Example 5. Finally, we consider the splitting of solitary wave

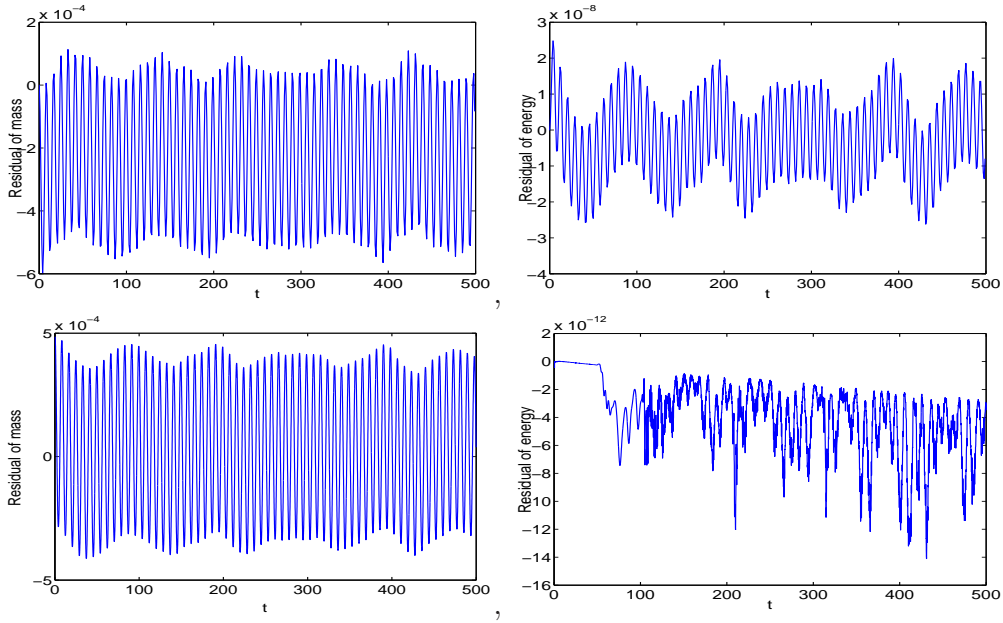


Figure 10: Conservative comparison. Upper for scheme (14), lower for scheme (32). Left for mass, right for energy.

$$\begin{cases} u_{tt} - u_{xx} + iu_t + |u|^2u = 0, & (x, t) \in [-40, 40] \times (0, 20], \\ u(x, 0) = (1 + i)x \exp(-10(1 - x)^2), & u_t(x, 0) = 0. \end{cases} \quad (36)$$

We simulate the problem by the MI (14) under the partition $h = 0.05, \tau = 0.02$. The residuals of mass and energy are reported in Fig. 11, and the profiles of the numerical solution are plotted in Fig. 12. From the pictures, it is observed that the original wave splits into some lower waves rapidly, and more and more ripples bring up with the evolution of wave. Both the mass and energy are nicely preserved.

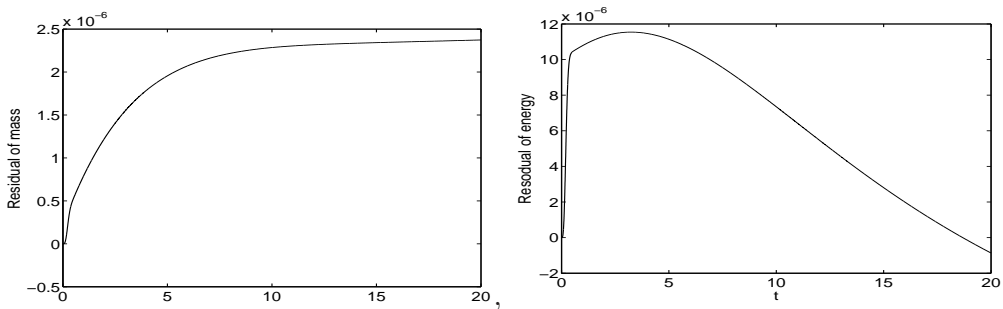


Figure 11: The residuals of mass (left) and energy (right).

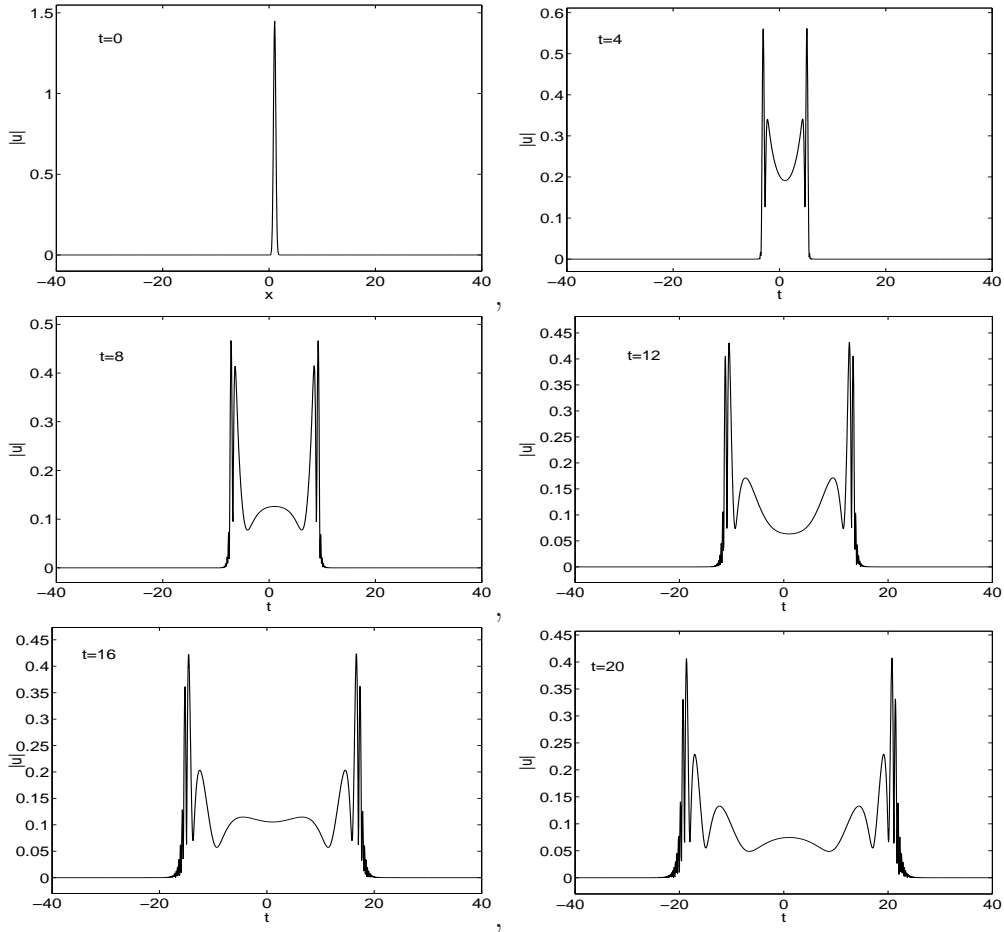


Figure 12: Profiles of the wave at different time stages.

6. Conclusion

In this study, we have used multisymplectic midpoint rule to approximate the Schrödinger equation with wave operator. The global conservative properties of the numerical method are investigated. For nonlinear problem, they usually do not keep the mass and energy exactly. However, their residuals are very small over long-term. The proposed numerical method demonstrates remarkable stable over long-term. Through numerical illustrations, it is observed that the numerical methods is more accurate than other energy-preserving methods.

Acknowledgement

This work is supported by the National Natural Science Foundation of China (Nos. 11271171, 11301234, 91130003), the Provincial Natural Science Foundation of Jiangxi (No. 20142BCB23009), the Foundation of Department of Education Jiangxi

Province (No. GJJ12174), the State Key Laboratory of Scientific and Engineering Computing, CAS, and Jiangsu Key Lab for NSLSCS (No. 201302).

References

- [1] Håvard Berland, Alvaro L. Islas b, Constance M. Schober, Conservation of phase space properties using exponential integrators on the cubic Schrödinger equation. *J. Comput. Phys.* 225 (2007) 284-299.
- [2] T.J. Bridges, S. Reich, Multi-symplectic integrators: numerical schemes for Hamiltonian PDEs that conserve symplecticity. *Phys. Lett. A.*, 284 (2001), 184-193.
- [3] B. Guo, H.X. Liang, On the problem of numerical calculation for a class of the system of nonlinear Schrödinger equation with wave operator. *J. Numer. Meth. Comput. Appl.* 4 (1983) 176-182
- [4] J. Hong, L. Kong, Novel multisymplectic integrators for nonlinear fourth-order Schrödinger equation with trapped term. *Commun. Comput. Phys.* 7 (2010) 613-630.
- [5] J. Hong, C. Li, Multi-symplectic Runge-Kutta methods for nonlinear Dirac equations. *J. Comput. Phys.*, 211 (2006), 448-472.
- [6] J. Hong, Y. Liu, Hans Munthe-Kaas, Antonella Zanna, Globally conservative properties and error estimation of a multi-symplectic scheme for Schrödinger equations with variable coefficients. *Appl. Numer. Math.*, 56 814-843(2006).
- [7] H. Huang, L. Wang, Local one-dimensional multisymplectic integrator for Schrödinger equation, *J. Jiangxi Normal. Univer.*, 35 (2011), 455-458.
- [8] A.L. Islas, C.M. Schober, Conservation properties of multisymplectic integrators. *Future Gen. Comput. Syst.* 22(2006) 412-422.
- [9] L. Kong, J. Hong, J. Zhang, Splitting multi-symplectic methods for Maxwell's equation, *J. Comput. Phys.*, 229 (2010)4259-4278.
- [10] K. Matsuuchi, Nonlinear interactions of counter-travelling waves. *J. Phys. Soc. Japan.* 48(1980) 1746-1754.
- [11] M. Qin, Y. Wang, Structure-preserving algorithm for partial differential equation. *Sci. & Tech. of Zhejiang publisher*, 2011.
- [12] S. Reich, Multi-symplectic Runge-Kutta collocation methods for Hamiltonian wave equation. *J. Comput. Phys.*, 157 (2000), 473-499.

- [13] J. Wang, Multisymplectic Fourier pseudospectral method for the nonlinear Schrödinger equation with wave operator. *J. Comput. Math.* 25(2007) 31-48.
- [14] L. Wang, Multisymplectic Preissman scheme and its application. *J. Jiangxi Normal Univer.* **33** (2009), 42-46.
- [15] Y. Wang, M. Qin, Multisymplectic structure and multisymplectic scheme for the nonlinear wave equation. *Acta. Math. Appl. Sinica*, 18(2002) 169-176.
- [16] S. Wang, L. Zhang, R. Fan, Discrete-time orthogonal spline collocation methods for the nonlinear Schrödinger equation with wave operator. *J. Comput. Appl. Math.* 235(2011) 1993-2005.
- [17] T. Wang, L. Zhang, Analysis of some new conservative schemes for nonlinear Schrödinger equation with wave operator. *Appl. Math. Comput.* 182(2006) 1780-1794.
- [18] L. Zhang, Q. Chang, A conservative numerical scheme for a class of nonlinear Schrödinger equation with wave operator. *Appl. Math. Comput.* 145(2003) 603-612.
- [19] H. Zhu, Y. Chen, S. Song, H. Hu, Symplectic and multi-symplectic wavelet collocation methods for two-dimensional Schrödinger equations. *Appl. Numer. Math.*, 61(2011), 308-321.